Energy Harvesting Utilizing Reciprocating Flow-Induced Torsional Vibration on a T-Shaped Cantilever Beam

Guangcheng Zhang[1,2], Christian Klumpner[1] and Yueh-Jaw Lin[2]

1. Department of Electrical and Electronic Engineering, University of Nottingham, Nottingham NG7 2RD, UK

2. Department of Mechanical, Materials and Manufacturing Engineering, University of Nottingham Ningbo China, Ningbo 315100, China

Abstract

This paper proposes a T-shaped cantilever energy harvester powered by flow-induced torsional vibration. To collect and convert the mechanical (kinetic) energy into electric power, a pair of symmetrical acrylic cylindrical bluff bodies were installed onto the bottom surface of the T-shaped cantilever beam, one at each end; There is also one patch of Macro Fibre Composite (MFC) used as an energy collector and converter which was attached to the fixed end of the cantilever beam. This proposed setup of the energy harvester is able to generate sustainable electric power by harvesting natural mechanical power resulted from the torsional vibration of the beam due to fluid's vortex shedding effects. The proposed energy harvester has the novelty in that our approach harvests fluid flow's energy in a reciprocal fashion making full use of renewable energy incurred in areas surrounding the two bluff bodies. Both the theoretical and experimental analyses on the proposed energy harvesting structure were performed and demonstrated in this paper. The case in the test rig we studied on the proposed energy harvester was able to generate sustainable electric power of approximately 1.0 μW when flow speed was measured to be 0.33 m/s flowing through two bluff bodies each of 29.5 mm diameter. This work also looks into and discusses pros

and cons of various scenarios in terms of structural geometric variations for system optimization of the proposed energy harvester.

Key points: T-shaped cantilever beam, energy harvester, reciprocating flow-induced torsional vibration, MFC

Introduction

Energy harvesting technology is a relatively small-scale prolific power generation method, compared with conventional power plants [1]. Over the past two decades, the study of energy harvesting have received more and more attention from scholars due to its potential applications [2-5], such as in wireless nodes system, in embedded devices, and in health monitoring technology, etc. There are many conversion principles which are mainly utilized in order to convert the ambient energy into electrical energy, namely, piezoelectricity, photovoltaic effect, electromagnetic induction mechanism and thermoelectric effect. Among the above mentioned conversion principles, piezoelectric-based technologies are regarded as a promising technology to increase the amount of renewable energy harvested, with special focus on micro power generation where there is a need to power sensors whilst it is impossible or uneconomical to fit a power cable (remote locations or in health applications) [6, 7].

The structure of the first proposed piezoelectric energy harvester consists of a cantilever beam with a mass at one end, and the other end of the cantilever beam is fixed with the vibration excitation[8]. The piezoelectric material is attached closely to the root of the cantilever beam, since the largest strain happens at that side when the harvester works in the bending mode. This kind of energy harvester works mainly in base excitation conditions. After that, many scholars have been focusing on enhancing the power output of the energy harvester; the principles, such as multimodal structures and resonance tuning

methods, are proposed and investigated [9-13]. The distribution of the strain along the cantilever beam is non-uniform, however, the strength of the beam will clearly be greatly affected. Besides that, the current proposed structure is strictly designed to be placed directly over the base vibration source, meaning that the practical applications of these kinds of energy harvesters are somewhat limited. In light of the above challenges, many scholars stated the structures working in torsional mode with base excitation. It is believed that the bandwidth and application range of these kinds of structure are tuned to be broader with torsional mode [14, 15].

Besides harvesting the energy from base vibration sources, several studies have recently been conducted on harvesting the energy from flow-induced vibration [16-18]. When a structure is subjected to flow loads in fluid-dynamic field, it may undergo various flow-induced responses, including vortex shedding vibration, flutter and galloping. These types of responses could be introduced into the energy harvesting technologies and converted into electrical power output. Different from the base excitation, to this kind of energy harvester, the mass at the tip undertakes the free end excitation directly; this acting form of the load could then induce higher strain at the fixed end of the energy harvester, compared to that with base excitation. In addition, due to the end of the cantilever beam being fixed, the absolute displacement of the whole structure with tip excitation is smaller than that of the base excitation. The most well-known flow-induced energy harvester consists of a cylinder attached to the free end of a cantilever beam and a patch of piezoelectric material is attached at the root of the cantilever in order to convert the kinetic power into electrical power, working in the bending mode [19]. The investigation of the improvement of the flow-induced energy harvesting technology have being conducted after this [20-22]. Most of the proposed energy harvesters, however, could only extract the flow energy from unidirectional flow, which limited the range of the application under complex flow conditions. In addition, most of the structures mainly work in the bending mode, which suffer the same strength problems with the former vibration-based energy harvesters.

In this paper, a cantilevered T-shaped flow-induced energy harvester is proposed. A pair of symmetrical acrylic cylinders are fixed on the bottom surface of the cantilever beam, one at each end, to induce the vibration from the water flow. One patch of MFC is attached at the root of the beam in order to convert the kinetic power into electrical power, regarding the direct piezoelectric effect. The harvester is powered by the flow-induced torsional vibration, which is excited by the vortex shedding from the interaction between the laminar water flow and the cylindrical bluff bodies. In concurrence with the previous studies on energy harvesting technologies, the torsional structure in this paper is referred to as a 'beam' rather than a 'bar'. Benefited with the symmetricity of the cantilever beam, the proposed energy harvester could harvest the flow energy from the reciprocating flow as well. With the utilization of the torsional mode, the distribution of the strain along the beam will then be uniform, which leads to higher efficiency of energy conversion. The capacitance of the piezoelectric patch will increase with an increase of the surface area. Regarding the uniform strain distribution of the energy harvester with the torsional mode, it is clear that the increase of the area of the piezoelectric patch is beneficial in improving the overall electrical power output. Considering the structural strength and stability of the torsional mode, the proposed energy harvester has more feasibility for practical application, compared to those working in the bending mode.

Structure and principle

Figure 1 shows the schematic figure of the proposed structure; the cylindrical bluff bodies are symmetrically connected to both the ends of T-type cantilever beam with the interference fit joint. The cross section formed by the centre lines of the inducing bluff bodies is parallel to the flow direction in the experimental system. The dimension of the bluff bodies is variable in the experimental measurement. The bluff bodies are made of acrylic material and the cantilever beam is made of pure copper with a 0.3 mm thickness. There is a piezoelectric patch (MFC, M2814-P2, Smart Materials Corp.) attached at the root of

the T-shaped cantilever beam in order to convert the kinetic energy from the water flow into electrical power.

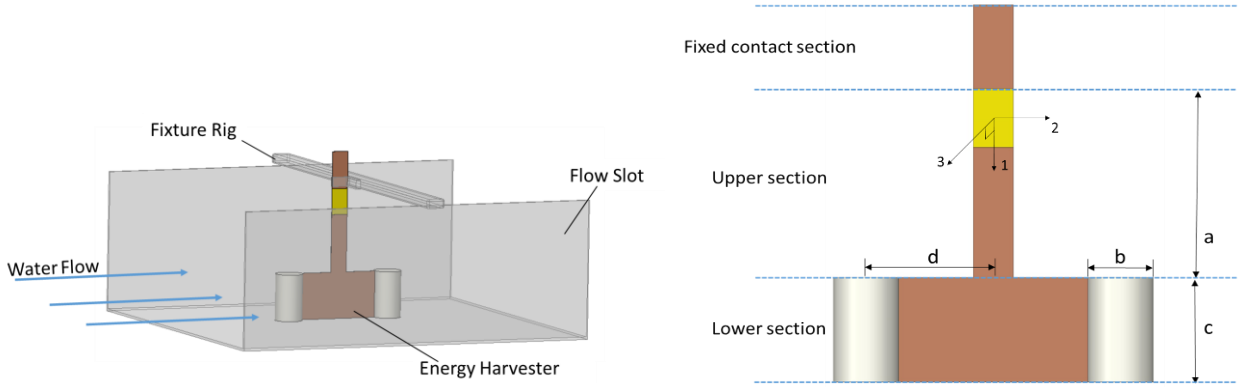

(a)

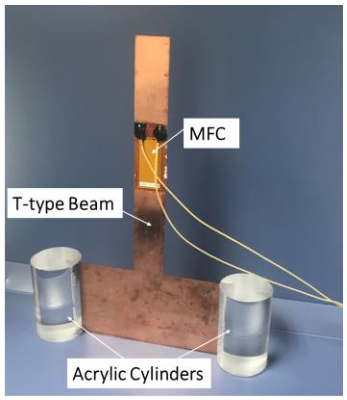

(b)

Figure 1. (a) Schematic diagram of a flow-induced energy harvester and (b) the photo of the prototype

Table 1 lists the geometric and material parameters of the MFC material and the energy harvester. The T-shaped cantilever beam is divided into three sections, as shown in Figure 1(a), in order to better explain the following parts. The fixed contact section is clamped by the fixture rig over the flow channel. For the following analytical parts, the upper side of the T-shaped cantilever beam will be considered as the bar

working in the pure torsional mode. The deformation on the lower section of the cantilever beam, and bluff bodies and their rotation are ignored, since the contribution of this paper is mainly on the analysis and validation of the fluid-structure interaction for the proposed structure.

MFC material is selected as the key piezoelectric component to convert the strain induced by the kinetic vibration into electric power based on direct piezoelectric effect, due to its high flexibility, reliability and damage-tolerance [23]. The key technology of the MFC is the fabrication of the piezoelectric macro fibre composite. It consists of making a piezoelectric fibre sheet by providing a plurality of wafers of piezoelectric material (piezoelectric ceramic), bonding the wafers together with an adhesive materials to form a stack of alternating layers of piezoelectric material and adhesive material, and cutting through the stack in a direction substantially parallel to the thickness of the stack and across the alternating layers of piezoelectric material and adhesive material to provide at least one piezoelectric fibre sheet having two sides comprising a plurality of piezoelectric fibres in juxtaposition to the adhesive material.[24]

The mechanical strain tensor **S** and the electric displacement **D** in the piezoelectric patch could be derived from the piezoelectric constitutive relationship as shown below [25, 26],

$$\begin{bmatrix} \boldsymbol{S} \\ \boldsymbol{D} \end{bmatrix} = \begin{bmatrix} \boldsymbol{S^E} & \boldsymbol{d} \\ \boldsymbol{d_t} & \boldsymbol{\varepsilon^T} \end{bmatrix} \begin{bmatrix} \boldsymbol{T} \\ \boldsymbol{E} \end{bmatrix} \tag{1}$$

Where **S** is the mechanical strain tensor, **T** is the mechanical stress tensor, $\mathbf{S^E}$, **d**, and $\boldsymbol{\varepsilon}^{\mathbf{T}}$ are the elasticity matrix, the inverse piezoelectric coefficient constant and the dielectric constant of the piezoelectric material, respectively. $\mathbf{d_t}$ is the piezoelectric coefficient tensor, which is normally same with **d** for the common piezoelectric materials.

In this paper, both surfaces of the MFC patch parallel to the cantilever beam are used as the electrode tips, and the poling direction is along the 3rd axis which is shown in Figure 1(a). The piezoelectric patch works in d_{31} mode and the piezoelectric equation could be simplified as,

$$D_3 = d_{31} T_1 \quad (2)$$

Where D_3 is the electric displacement between the electrode tips, d_{31} is the piezoelectric constant where the subscripts 3 and 1 respectively denote the polarization direction and the applied force direction, and T_1 is the stress along the 1st axis induced by the restrained torsional response of the MFC patch.

Table 1. The geometric and material parameters of the MFC material and the energy harvester.

Parameters	Values
D_{31} (pC/N)	-2.1E02
Capacitance of MFC (nF)	35
Tensile modulus of MFC (GPa)	15.857
Shear modulus of MFC (GPa)	5.515
The width of the MFC (mm)	14
The length of the MFC (mm)	28
Mass density of the beam (kg/m^3)	8900
Tensile modulus of the beam (Gpa)	110
Shear modulus of the beam (Gpa)	40
Shear modulus of the beam (Gpa)	40
The length of line a (mm)	80
The diameter of the cylinders b (mm)	29.5
The length of line c (mm)	50
The length of line d (mm)	47.5
Mass density of the beam (kg/m^3)	8900
Mass density of the bluff bodies (kg/m^3)	1180

According to the vortex shedding theory in fluid dynamic analysis, if the laminar fluid flow through the surface of the cylindrical bluff body, the body experiences a pressure difference between the both surfaces of the body, based on the alternative shedding of the vortex [27, 28]. The bluff body converts the kinetic energy of the uniform and steady fluid flow into large temporal pressure fluctuations caused by vortex shedding. Based on the above, the mechanical forces from shedding vortices are exerted directly onto the beam through the inducing bluff bodies with the proposed structure, and the torsional mode could then be induced. Figure 2 shows the free body diagram of the structure. L_1 and L_2 are the induced lift forces from the interaction between the laminar water flow and the cylindrical bluff bodies, D_1 and D_2 are the drag forces (in this paper, the response of the drag forces will not be discussed). The value of the lift force is normally calculated based on the analysis of Reynolds-stress tensor in fluid mechanics and experimental fluid mechanics [29]. It is believed that the proposed structure will work in the coupled bending-torsion vibration, the normal strain from the bending mode should also play a role on the power conversion. However, based on the observation of the experimental test, the torsional vibration is the dominant vibrational mode of the proposed energy harvester. Hence, in this paper, the phase difference of the lift forces is assumed to be 180^o and the values of those are same with each other. Based on the above explanation and simplification, since the centreline of the structure corresponds to the centre of the gravity, the proposed energy harvester works mainly in torsional mode.

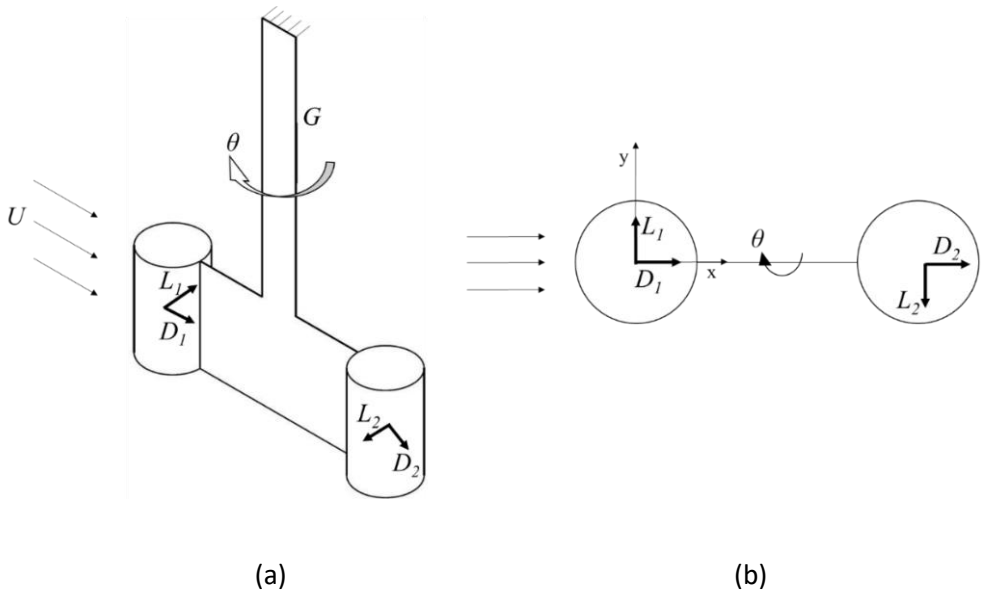

(a) (b)

Figure 2. (a) Free body diagram of the structure of the energy harvester (b) Top view

According to the direct piezoelectric effect, the electrical power could be tested from the MFC material when the energy harvester works in the torsional mode. The piezoelectric circuit model (i.e. the voltage generator connected to a capacitor and a resistance in series) is utilized in the model to analyse the output of the energy harvester [30]. The open-circuit output voltage generated by the energy harvester was captured across the DAQ (Data Acquisition, PCI8640, Art-control Corp.). The average output power P_{av} transferred to a load resistor can be calculated by:

$$P_{av} = \frac{1}{T}\int_0^T \frac{V(t)^2}{R_L} dt = \frac{V_{rms}^2}{R_L} \quad (3)$$

where V_{rms} is the root mean voltage across the load resistor R_L. P_{av} reaches the maximum when R_L equals its optimal value [31, 32]:

$$R_{Lo} = \frac{\sqrt{1+(\omega C_P R_P)^2}}{\omega C_P} \quad (4)$$

where ω is the vibration frequency of the energy harvesting module and C_P is the capacitance of the MFC material. For an ideal piezoelectric model, the internal resistance R_p is equal to zero. Equ. (4) will be used to estimate and define the optimal load resistors at different operating frequencies later in the test.

Assuming that the energy harvester generates a sinusoidal voltage, the voltage source is equal to the open circuit voltage. The average output power P_{av} transferred to a load resistor can be calculated by:

$$P_{av} = \frac{V_{oc}^2}{2R_L[1+(1/\omega C_p R_L)^2]} \quad (5)$$

where V_{oc} is the peak open circuit voltage.

In the following parts of the paper, Equ. (4) was used to estimate the optimal resistance in the working conditions and the electric power of the energy harvester was tested by the circuit load as well to validate the numerical result.

Experimental setup

Figure 3 shows the setup of the experimental system. [20, 33] The whole system consists of two water tanks, pumps, flow meters, a flow channel, diffusers, and inlet and outlet pipes. The water flows into the tank on the left through pumps firstly, and then passes through two layers of diffusers to develop. The flow rates of the inlet and outlet pipes were the same, and the length of the flow channel was approximately two meters, which ensured that the water flow was fully developed into the laminar flow. The central part of the flow channel is utilized in the experiment to deploy the energy harvester. The open-circuit output voltage generated by the energy harvester was captured across the DAQ. The width of the flow channel was 31.5 cm. The flow rate was read through the flow meters, and the speed of the flow could be calculated by:

$$V=Q/S \tag{6}$$

where V is the flow speed in the flow channel, Q is the flow rate, and S is the area of the cross section of the flow domain.

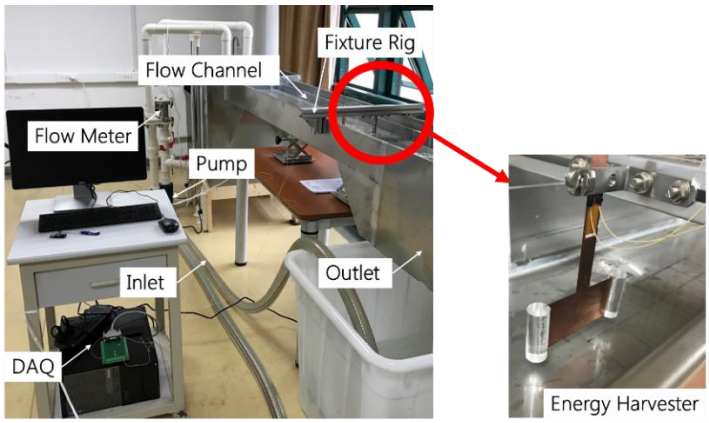

Figure 3. Setup of the experimental system.

Due to the limitation of the pump and the dimension of the flow channel, the maximum water flow rate was 32 m^3/h. It was estimated that the range of the water flow speed was from 0 to 0.33 m/s when the depth of the water flow was restricted to 80 mm.

Response analysis in torsional mode

The governing equation of the torsional vibration for this flow-induced energy harvester is given by:

$$I\ddot{\theta} + C\dot{\theta} + k\theta = M \tag{7}$$

Where *I* is the mass moment of inertia to the respect of the centreline of the lower section, *G* is the shear modulus of the upper section, k is the torsional stiffness of the upper section and $k = GJ/a$, *J* is the second

moment of the beam to the respect of the centreline, *M* is the external torque caused by the mechanical forces from shedding vortices. The torsion centre locates at the centreline of the structure. It is easily understood that the strain on the MFC would increase along with an increase in angle of twist θ, the electric power it generated would increase.

Based on the former studies on fluid flowing through circular cylinder in two-dimensional method [34], the net force on the body from the fluid could be expressed as,

$$\boldsymbol{F} = -\rho \frac{d}{dt} \int_{whole\ fluid} \boldsymbol{u} d\boldsymbol{x} = -\frac{d}{dt} \int_{whole\ domain} \boldsymbol{u} d\boldsymbol{x} + \frac{d}{dt} \int_{body} \boldsymbol{u} d\boldsymbol{x} \tag{8}$$

When the definition of vorticity is substituted into Equ (6),

$$\boldsymbol{F} = -\rho \frac{d}{dt} \int_{whole\ fluid} (\boldsymbol{\omega} \times \boldsymbol{x}) d\boldsymbol{x} + \rho S \frac{d\boldsymbol{U}}{dt} \tag{9}$$

where ρ is the density of the fluid, $\boldsymbol{\omega}$ is the vorticity, $\boldsymbol{x}$ is the location, *S* is the area of the body and $\boldsymbol{u}$ is the velocity.

Hence, the lift on the bluff body could be expressed as,

$$\boldsymbol{L} = \boldsymbol{F} \cdot \hat{\boldsymbol{e}}_{\boldsymbol{y}} \cdot c \tag{10}$$

The applied moment due to the loading conditions can be expressed as,

$$M = Ld \tag{11}$$

Where L is the mechanical force from shedding vortices. The vortices shed from the bluff body alternatively and regularly, due to the vortex shedding theory [27]. The effective moment acting on the structure is given by,

$$M = Ld = A\sin(2\pi f_s t) \tag{12}$$

Where A is the max moment exerted on the structure and f_s is the shedding frequency of the vortex after bluff body.

The empirical Strouhal number with the given wake thickness and free stream velocity is conducted to determine the vortex shedding frequency of the inducing bluff bodies [35, 36]:

$$S_t = f_s b/U \tag{13}$$

where f_s is the vortex shedding frequency and f_s has unites of *Hz* here, b is the diameter and U is the speed of the inlet flow.

For the harmonic excitation from vortex-induced vibration, the solution of the θ to the Equ (7) is

$$\theta(t) = \bar{\theta}\sin(2\pi f_s t - \varphi) \tag{14}$$

Where $\bar{\theta}$ is the amplitude and $\bar{\theta} = \frac{A}{J\omega_n^2\sqrt{[1-(\frac{2\pi f_s}{\omega_n})^2]^2+4\zeta^2(\frac{2\pi f_s}{\omega_n})^2}}$, φ is the phase angle and $\varphi = \tan^{-1}\frac{2\zeta(\frac{2\pi f_s}{\omega_n})}{1-(\frac{2\pi f_s}{\omega_n})^2}$. ω_n is the natural frequency of the torsional vibration and $\omega_n = \sqrt{\frac{GJ}{Ia}}$; ζ is the damping ratio and $\zeta = \frac{C}{2\omega_n J}$.

The excitation of the torsional vibration happens when the excitation frequency equals natural frequency and the amplitude of the response is

$$\bar{\theta} = \frac{A}{2J\omega_n^2\zeta} \tag{15}$$

Based on the above analysis, the torsional response of the proposed flow-induced energy harvester is related with the parameters of the material, the length of the line d and the shedding frequency. The characteristics of the energy harvester would be shown in the discussion section.

Experimental results and simulation

The output characteristics of the prototype were tested and processed in this study. The open-circuit voltage output of the prototype is shown in Figure 4. In this experimental measurement, the flow speed was set as 0.33 m/s, the diameter (b) of the bluff bodies was 29.5 mm and the width (2d) of the lower section was 95 mm.

It is shown in Figure 4 that a stable and sustained power output could be extracted from the laminar water flow. The root mean square of the peak open circuit voltage was approximately 3.2 V, and the frequency of the generated AC signal was around 1.8 Hz. The estimated optimal resistance could be calculated when the signal frequency is substituted into Equ. (4). The numerical and experimental results of the output power P_V is shown in Figure 5. It shows that the optimal resistance of this energy harvester without power conditioning is around 2.5 MΩ and the maximum output of the energy harvester at the setup condition could reach 1.03 μW.

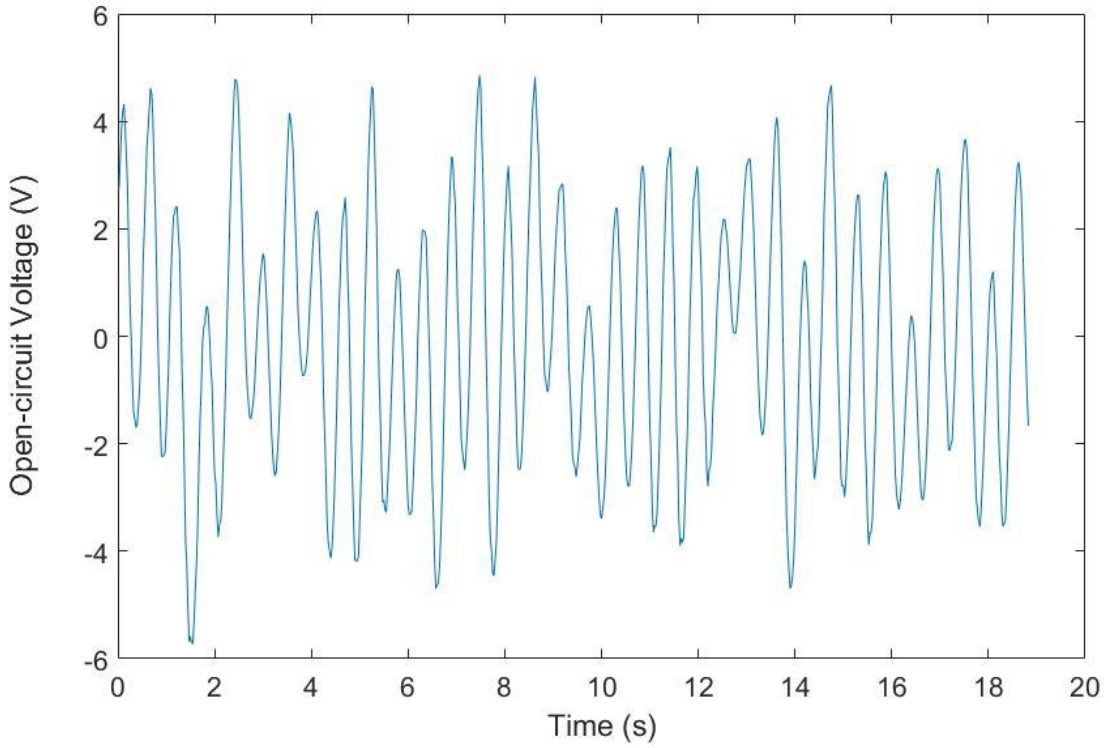

Figure 4. Relationship between open-circuit voltage and flow time

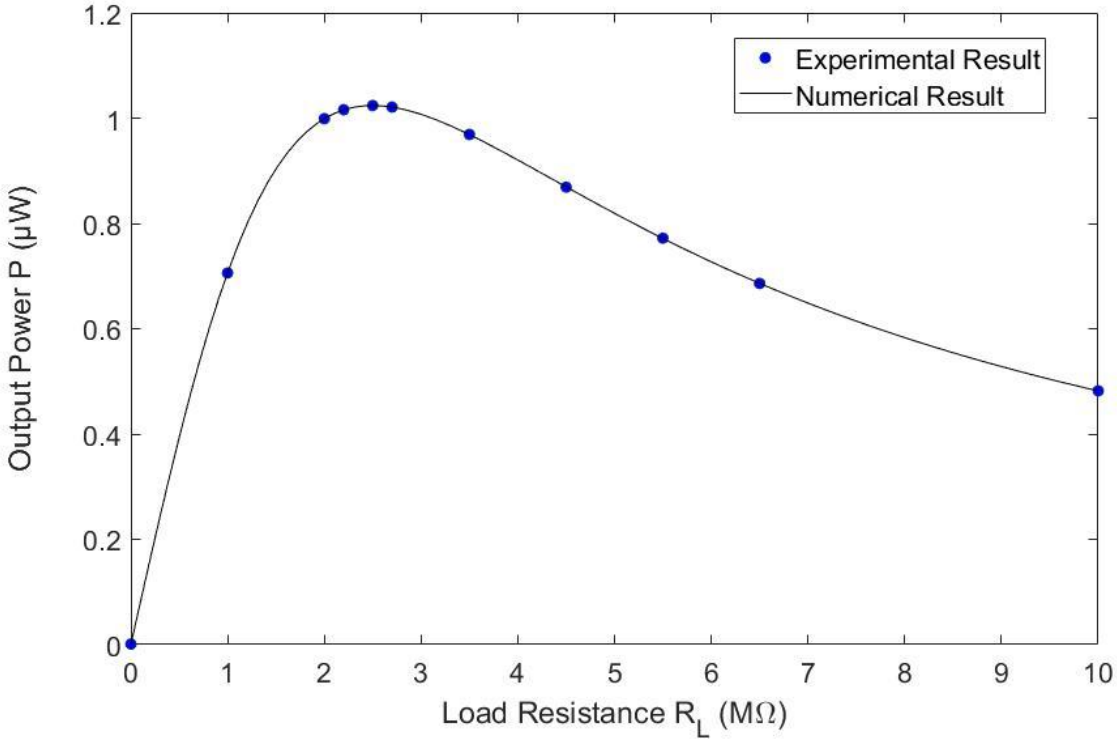

Figure 5. Numerical and experimental results of the output power P versus the load resistance R_L

It can be clearly seen that they are both in strong agreement with each other in the electrical aspect. In the following sections of the paper, the proposed methods will be utilized to estimate the output power of the energy harvester with variable parameters.

In order to explain the working condition of the prototype, a finite element software (Ansys) is used to simulate the vibration of the energy harvester. The FEM model of the structure is shown in Figure 6 and the torsional vibration mode is shown in Figure 7. It demonstrates that the frequency of the first-order torsional mode of the structure is 3.3 Hz. Besides that, the modal analysis also shows that the frequency of the first-order and second-order bending modes are 1.7 Hz and 18 Hz respectively. The frequency gap between the first bending and torsional modes is relatively narrow compared with that between the higher order vibration modes. Considering the shedding frequency of the vortex shedding, it is easily understood that the cantilever beam of the prototype undergoes the coupled bending-torsional vibration. With regards to both the excitation condition and structure design, the torsional mode is more easily excited and plays a dominant role in the vibration based on the experimental observation.

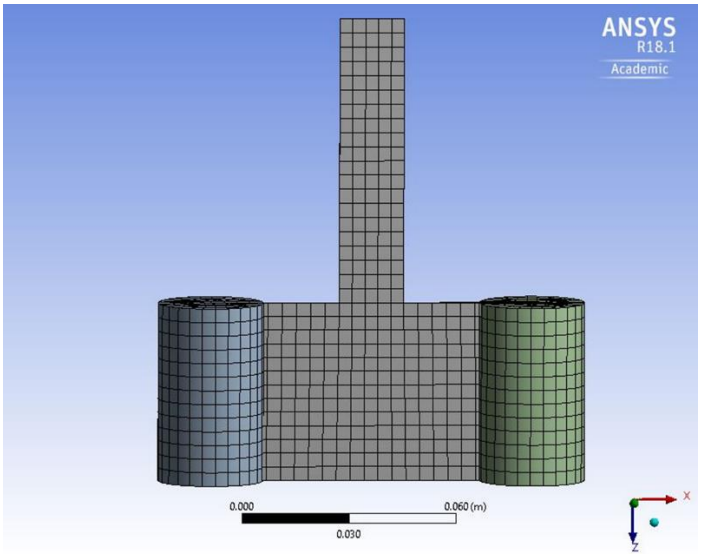

Figure 6. The model of FEM calculation

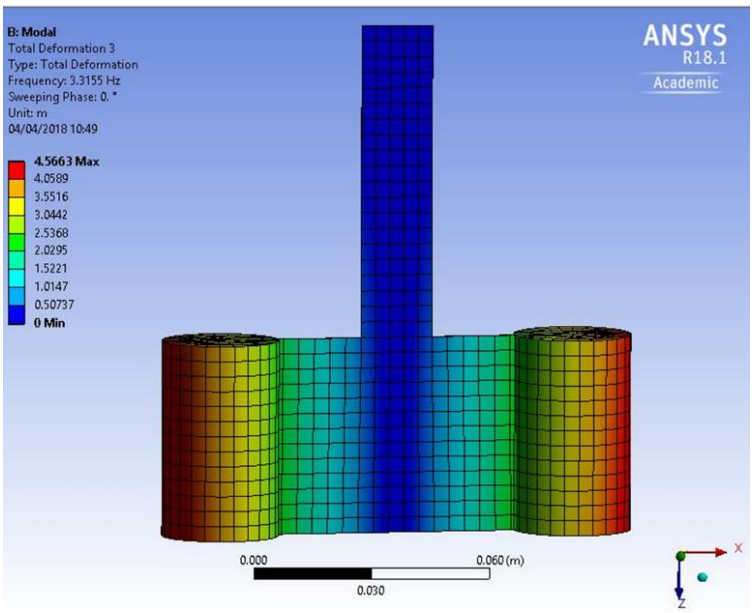

Figure 7. Torsional vibration mode calculated by the FEM

Figure 8 shows the strain distribution of the prototype. When it works in the torsional mode, it is obvious that the strain distribution of the torsional mode is more uniform than that of the bending mode. In the bending mode vibration, the highest strain will only occur at the root of the cantilever beam and the efficiency of the energy conversion will be lower. Besides this, the power output of the energy harvester working in the bending mode will not improve greatly with the increase of the area of the piezoelectric patch. The capacitance of the MFC will increase with an increase in area, based on the characteristics of MFC. Regarding the uniform distribution of the energy harvester with the torsional mode, it is clear that the increase of the area of the piezoelectric patch is beneficial to the electrical power output.

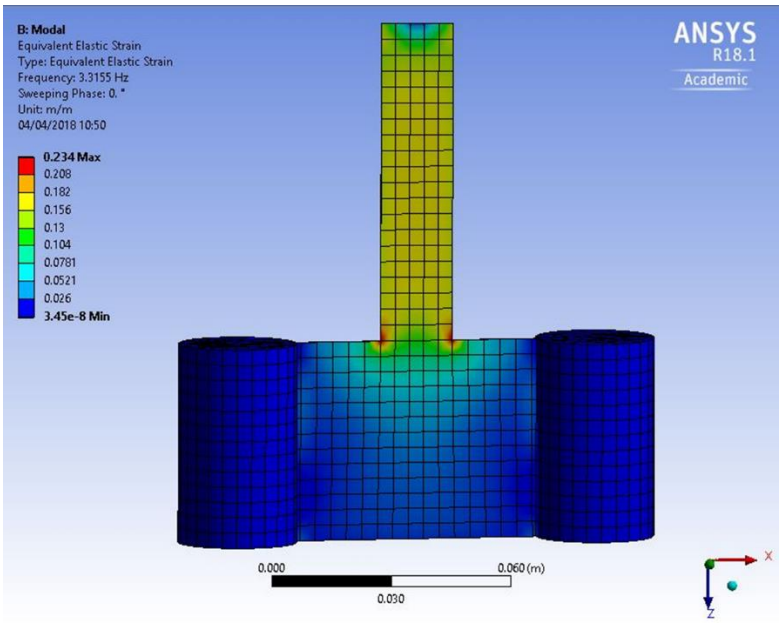

Figure 8. The strain distribution calculated by the FEM

Characteristics and discussions

As shown in Equ. (5), it is believed that the output power of the energy harvester is mainly related to the amplitude of the output signal and its power frequency. In order to investigate the characteristics of the energy harvester with a fixed width (2d = 95 mm), the speed response characteristics of the energy harvester were measured with bluff bodies of five different diameters: namely 9.85 mm, 14.3 mm, 19.5 mm, 24.8 mm and 29.5 mm (seen in Figure 9). Figure 9 shows that the output of this underlying structure increased along with an increase in flow speed, and that the flow speed was a critical influence on the output of the energy harvester - the higher the speed, the greater the output power. It can be understood that with an improvement in flow speed, the energy from the water flow would be higher, and the energy extracted from the flow would be increased as well.

Due to the limits of the flow rate, the largest flow speed that the laminar water flow system could generate was 0.33 m/s, but it can be predicted that the output would be greater at higher speeds. Figure 9 also shows that increasing the dimension of the inducing bluff bodies could help improve the output of the

proposed energy harvester. This can be explained in two parts: firstly, with the increase of the diameter of the bluff bodies, their weight will increase, and the torsional mode frequency of the whole structure will decrease based on the vibration theory; hence, the torsional mode is more easily excited. Secondly, the increase of the dimensions could undertake more energy from the water flow. It is believed that there is an optimal size for the bluff bodies within the proposed structure, where the structure could work in the resonant torsional mode at a certain range of the flow speed, and the output power will improve as a result.

The influence of the flow speed and the size of the bluff bodies on the frequency response is shown in Figure 10. It shows that signal frequency increases with an increase in flow speed. In general, the flow speed has a significant effect on the output frequency of the energy harvester. Based on the Strouhal number, the shedding frequency of the vortex street is proportional to the flow speed and is inversely proportional to the diameter of the bluff bodies. The experimental results also verified the theory. It was noticed that the frequency of the proposed energy harvester experienced a rapid increase when the flow speed was 0.3 m/s. From the above analysis, it was believed that the harvester worked in a complicated environment where the flow distribution around the harvester kept changing with the dynamic vibration of the T-shaped cantilever beam, the frequency response of the harvester was determined by the interaction between them. One possible explanation is that the response frequency is one of the resonant frequencies of the harvester, the resonant excitation of the energy harvester is easily excited around that range of the flow speeds, hence, the frequency fast raised up at the speed 0.3 m/s and stayed the same at 0.33 m/s as well.

As shown in Figures 9 and 10, the output power of the experimental results generally corresponds to the previous analysis, which cross-verified the analysis in the above parts as well. Besides undertaking the excitation from the water flow, the bluff located at the downstream flow could ensure that the topology

of the energy harvester is symmetrical, which could not only play a role in torsional vibration but could also make the energy harvester available with the reciprocating flows. From the above analysis, the mechanical forces from shedding are assumed to exert directly onto the bluff body and that there is no phase difference between the excitations on both bluff bodies. Besides this, the aerodynamic moments (Ma) developing on the tip body are assumed to be exerted directly onto the beam rather than being captured from the wake. It is believed that the flow condition for the bluff body located at the upstream flow is better than for the one at the downstream flow, and that the downstream one will work in the wake of the upstream one, which may affect the outcome of the energy harvester in practical applications.

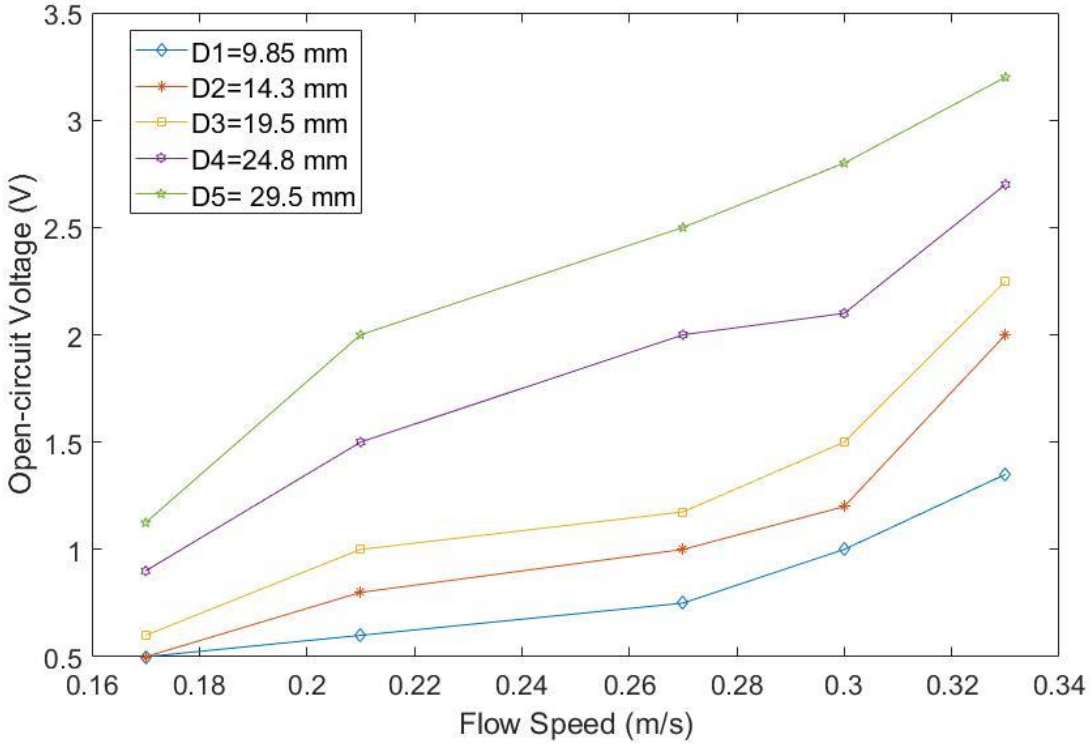

Figure 9. Relationship between peak open circuit voltage and diameters of the bluff bodies

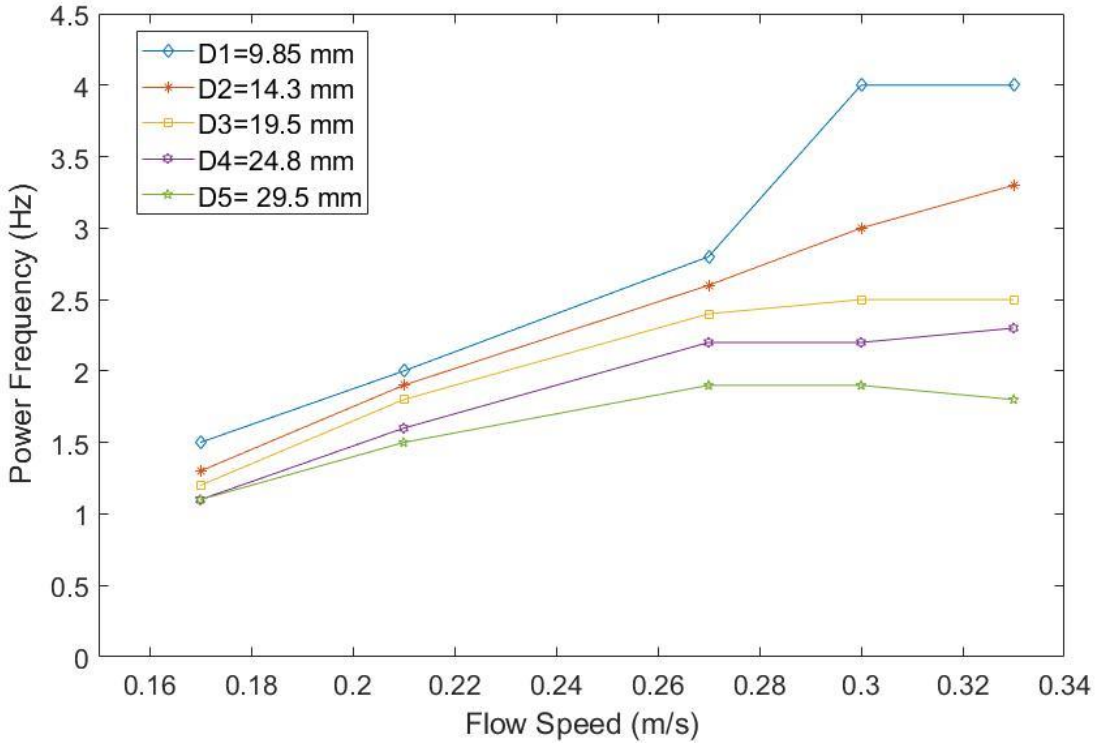

Figure 10. Relationship between output power frequency and diameters of the bluff bodies

The structures with variable dimensions of width (2d) are tested to investigate the output characteristics of the proposed energy harvester. Figure 11 shows the open-circuit voltage and frequency responses versus the flow speeds, with different dimensions of bluff bodies.

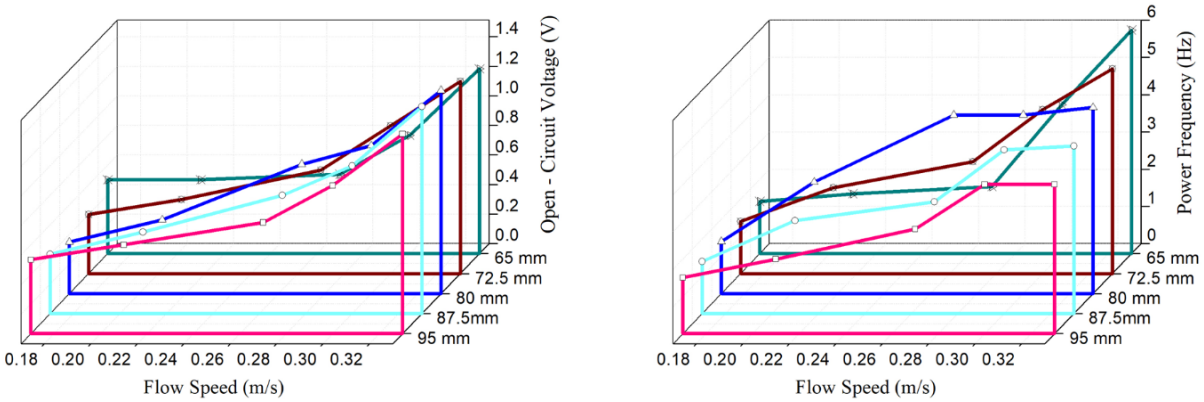

(a)

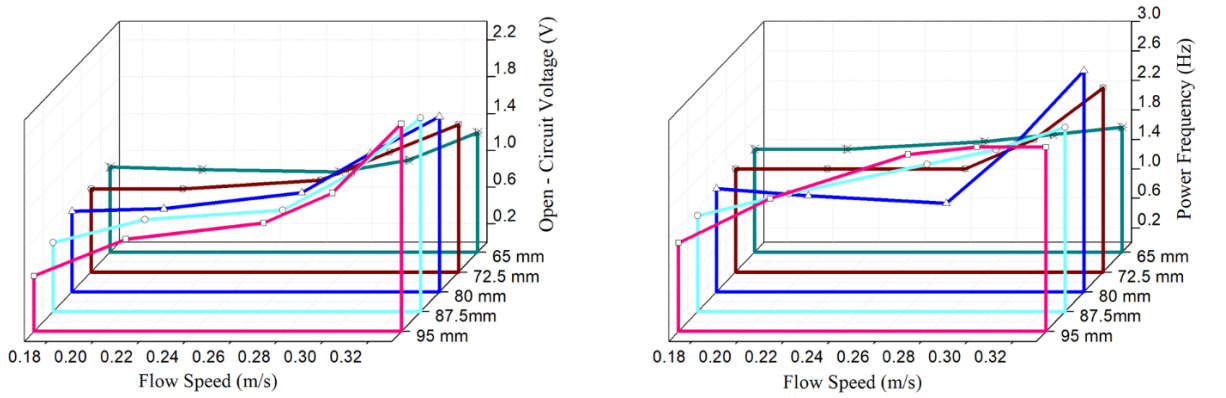

(b)

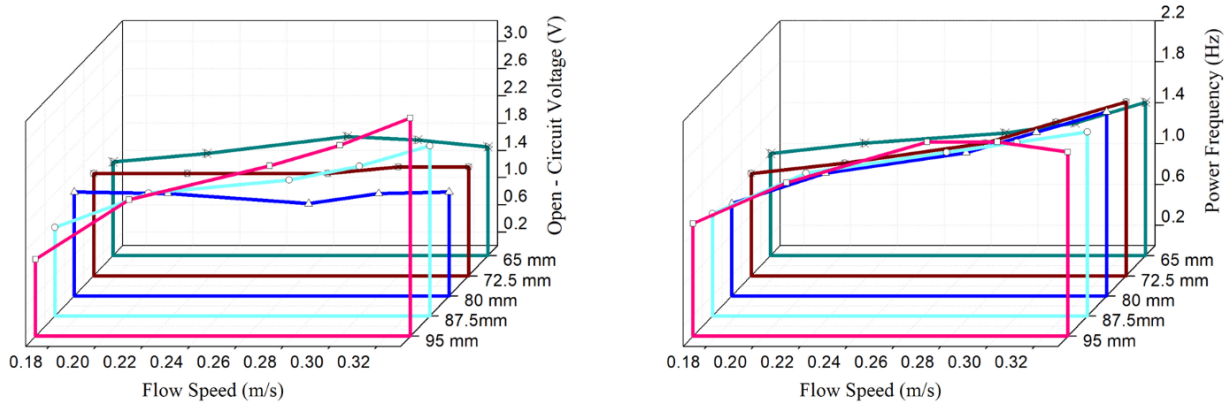

(c)

Figure 11. The voltage and frequency output of the energy harvester with different dimensions of the width of the lower section at the conditions of variable diameters (D) of the bluff bodies. (a) D = 9.85 mm (b) D = 19.5 mm (c) D = 29.5 mm

Figure 11 also shows that the output voltage increased with an increase of the flow speed in general. The frequency of the signal is not significantly related to the width of the lower section, it also cross verified the analysis. However, the open-circuit voltage increased with an increase in the width of the lower section of the energy harvester. In addition, the output frequency of the signal reached 6 Hz when the flow speed was 0.33 m/s, the width of the lower section was 65 mm and the diameter of the bluff was 9.85 mm. It is believed that the energy harvester was working in the resonant vibration. As discussed in

the previous sections, the power output of the proposed structure is related to both the voltage output and the signal frequency. In future research, the geometry optimization of the T-shaped cantilever beam and the bluff bodies will be investigated, based on the previous discussion to improve the output of the proposed flow-induced energy harvester. It is expected that the criteria of the design of the energy harvester at certain flow speeds could be figured out.

From the above figures, it can be observed that the dimensions of the bluff bodies have more effect on the voltage output of the energy harvester when the width of the lower section is relatively wide. In addition, the frequency response could be more significantly affected by the dimensions of the bluff bodies when the lower section is relatively narrow.

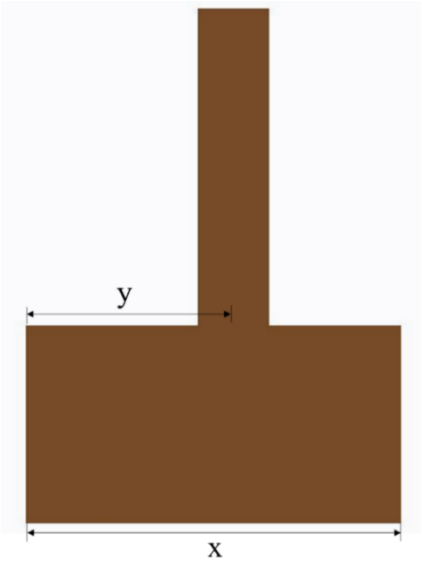

Figure 12. Schematic diagram of the ASYMM energy harvester

In addition to the study of symmetrical structure, the paper also included the work on the left-right asymmetrical layout of the lower section. In order to compare the results of previous experiments, the width of the lower section is manufactured at 95 mm as well (as shown in Figure 12). It is believed that the manufacturing cost of the structures is similar. The length between the left edge and the centreline

of the upper section (y) is 10 mm longer than the right one. The structure is named as left-asymmetrical if the longer side locates at the upstream. Likewise, the structure is known as right-asymmetrical if the shorter side locates at the upstream. Figures 13 shows the voltage and frequency response of the left-right asymmetrical structures under different working conditions, and the characteristics of the symmetrical ones are also shown.

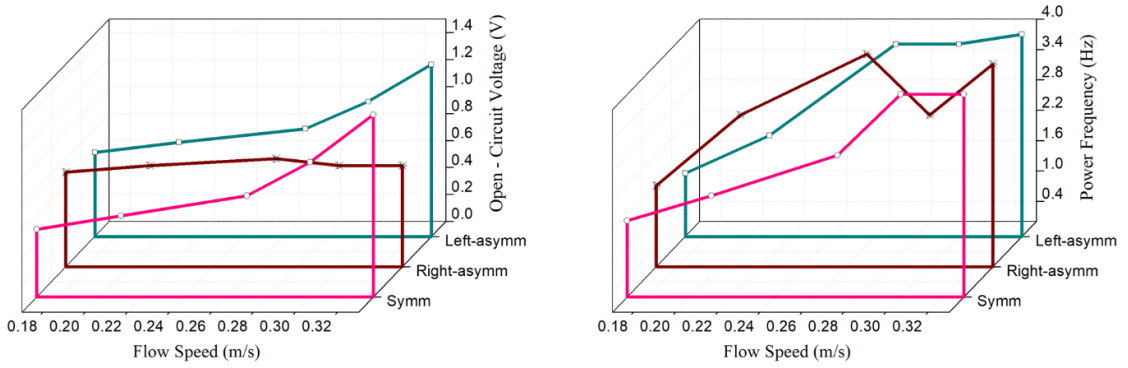

(a)

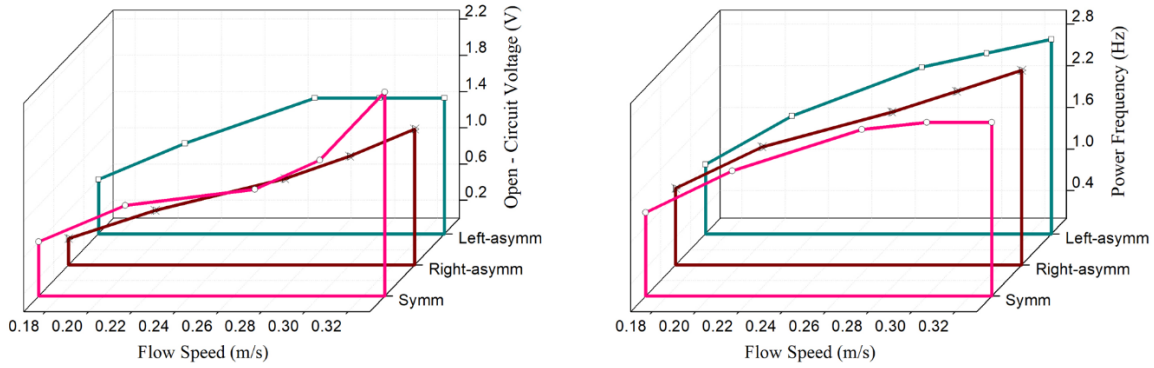

(b)

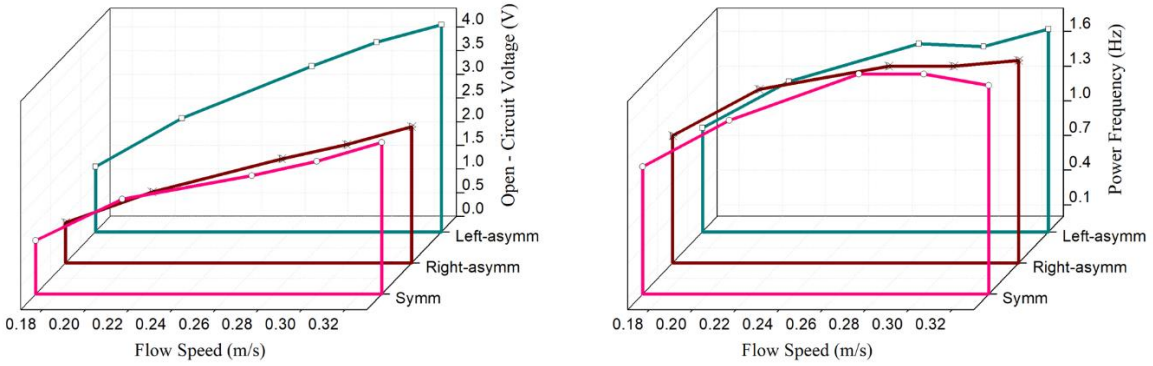

(c)

Figure 13. The voltage and frequency output of the ASYMM and SYMM energy harvesters at the conditions of variable diameters (D) of the bluff bodies. (a) D = 9.85 mm (b) D = 19.5 mm (c) D = 29.5 mm

Figure 13 shows that the output of the left-right asymmetrical structure is similar to that of the symmetrical structure on the frequency response part. The voltage response of the left-asymmetrical one, however, increased rapidly at higher speed, and the voltage response of the right-asymmetrical one was lower than that of the symmetrical one. If the energy harvester is expected to be utilized in the reciprocating flow condition, the symmetrical one could generate higher power and the vibration of the energy harvester could be regarded as the pure torsional mode. If the energy harvester is designed for the directional flow condition, the left-asymmetrical structure could be more beneficial for the power output; and it was also observed that the structure works in the bending-torsional mode in the experiment.

In future, the optimization of the energy harvester will be discussed, and the criteria of the design of the flow-induced energy harvester with torsional vibration will be discussed and analyzed in future studies. It is also believed that with the implementation of power conditioning, the efficiency of the electrical power output of the proposed energy harvester could also be improved.

Conclusion

In this paper, a newly proposed flow-induced energy harvesting approach was demonstrated. A pair of symmetrical acrylic cylindrical bluff bodies were fixed to the bottom surface of the T-shaped cantilever beam, one at each end, and one patch of MFC was attached at the root of the beam in order to convert the kinetic power into electrical power. The torsional vibration of the proposed structure was induced by the vortex shedding on the surfaces of the bluff bodies when the laminar fluid flows through them. The fact that this flow-induced energy harvester takes advantage of capturing the flow power from the reciprocating flows is a newly found development of flow-induced energy harvester never being brought up in the recent literature. Analytical modelling and experimental verification were both performed in this work to explain and prove the concept using the results of the paper. Based on the above discussion, the exciting force exerts directly on the mass tips, rather than on the fixed end. The energy harvester has a wider range of practical applications, compared with the base excitation structures developed in our earlier work. The strain distribution on the cantilever beam with torsional mode is more uniform, allowing us to improve the output of the harvested power through increasing the surface area of the piezoelectric patch. The strength of the proposed structure working in the torsional mode is higher than that in the bending mode. This implies that the lifespan of the structure will also be extended. In future studies, we will consider optimizing the energy harvester leading to improved voltage output and signal frequency in order to increase the power output. In addition, an optimized circuit model will be studied along the same line for generating more electrical power.

Acknowledgements

The author acknowledges the financial support from the International Doctoral Innovation Centre, Ningbo Education Bureau, Ningbo Science and Technology Bureau, and the University of Nottingham. This work was also supported by the UK Engineering and Physical Sciences Research Council [grant numbers EP/G037345/1 and EP/L016362/1]

References

1. Roundy, S., P.K. Wright, and J. Rabaey, *A study of low level vibrations as a power source for wireless sensor nodes.* Computer communications, 2003. **26**(11): p. 1131-1144.
2. Paradiso, J.A. and T. Starner, *Energy scavenging for mobile and wireless electronics.* IEEE Pervasive computing, 2005. **4**(1): p. 18-27.
3. Shaikh, F.K. and S. Zeadally, *Energy harvesting in wireless sensor networks: A comprehensive review.* Renewable and Sustainable Energy Reviews, 2016. **55**: p. 1041-1054.
4. Liu, M., et al., *Design, simulation and experiment of a novel high efficiency energy harvesting paver.* Applied Energy, 2018. **212**: p. 966-975.
5. Liang, J., Y. Zhao, and K. Zhao, *Synchronized Triple Bias-Flip Interface Circuit for Piezoelectric Energy Harvesting Enhancement.* IEEE Transactions on Power Electronics, 2018. **PP**(99): p. 1-1.
6. Sodano, H.A., D.J. Inman, and G. Park, *A Review of Power Harvesting from Vibration Using Piezoelectric Materials.* The Shock and Vibration Digest, 2004. **36**(3): p. 197-205.
7. Beeby, S.P., M.J. Tudor, and N.M. White, *Energy harvesting vibration sources for microsystems applications.* Measurement Science and Technology, 2006. **17**(12): p. R175-R195.
8. Roundy, S. and P.K. Wright, *A piezoelectric vibration based generator for wireless electronics.* Smart Materials and structures, 2004. **13**(5): p. 1131.
9. Zhang, G. and J. Hu, *A Branched Beam-Based Vibration Energy Harvester.* Journal of Electronic Materials, 2014. **43**(11): p. 3912-3921.
10. Li, P., et al., *A magnetoelectric energy harvester and management circuit for wireless sensor network.* Sensors and Actuators, A: Physical, 2010. **157**(1): p. 100-106.
11. Wei, C. and X. Jing, *A comprehensive review on vibration energy harvesting: Modelling and realization.* Renewable and Sustainable Energy Reviews, 2017. **74**: p. 1-18.

12. Priya, S., et al., *A Review on Piezoelectric Energy Harvesting: Materials, Methods, and Circuits*, in *Energy Harvesting and Systems*. 2017. p. 3.

13. Zhou, S. and L. Zuo, *Nonlinear dynamic analysis of asymmetric tristable energy harvesters for enhanced energy harvesting.* Communications in Nonlinear Science and Numerical Simulation, 2018. **61**: p. 271-284.

14. Gao, S., et al., *Study on characteristics of the piezoelectric energy-harvesting from the torsional vibration of thin-walled cantilever beams.* Microsystem Technologies, 2017. **23**(12): p. 5455-5465.

15. Abdelkefi, A., et al., *An energy harvester using piezoelectric cantilever beams undergoing coupled bending–torsion vibrations.* Smart Materials and Structures, 2011. **20**(11): p. 115007.

16. Abdelkefi, A., *Aeroelastic energy harvesting: A review.* International Journal of Engineering Science, 2016. **100**: p. 112-135.

17. McCarthy, J., et al., *Fluttering energy harvesters in the wind: A review.* Journal of Sound and Vibration, 2016. **361**: p. 355-377.

18. Zakaria, M.Y., M.Y. Al-Haik, and M.R. Hajj, *Experimental analysis of energy harvesting from self-induced flutter of a composite beam.* Applied Physics Letters, 2015. **107**(2): p. 023901.

19. Akaydin, H., N. Elvin, and Y. Andreopoulos, *The performance of a self-excited fluidic energy harvester.* Smart materials and Structures, 2012. **21**(2): p. 025007.

20. Zhang, G. and Y.-J. Lin, *A nonlinear flow-induced energy harvester by considering effects of fictitious springs.* Materials Research Express, 2017.

21. Deivasigamani, A., et al., *Piezoelectric energy harvesting from wind using coupled bending-torsional vibrations.* Modern Applied Science, 2014. **8**(4): p. 106.

22. Lin, Z., et al., *Asymmetric arc-shaped vortex-induced electromagnetic generator for harvesting energy from low-velocity flowing water.* IET Renewable Power Generation, 2017. **11**(12): p. 1503-1508.

23. Upadrashta, D. and Y. Yang, *Experimental investigation of performance reliability of macro fiber composite for piezoelectric energy harvesting applications.* Sensors and Actuators A: Physical, 2016. **244**: p. 223-232.

24. High, J.W. and W.K. Wilkie, *Method of fabricating NASA-standard macro-fiber composite piezoelectric actuators.* 2003.

25. *Publication and Proposed Revision of ANSI/IEEE Standard 176-1987 "ANSI/IEEE Standard on Piezoelectricity".* IEEE Transactions on Ultrasonics, Ferroelectrics, and Frequency Control, 1996. **43**(5): p. 717.

26. Feng, Q., et al., *Theoretical modeling and experimental validation of a torsional piezoelectric vibration energy harvesting system.* Smart Materials and Structures, 2018. **27**(4): p. 045018.

27. C.H.K. Williamson, a. and R. Govardhan, *VORTEX-INDUCED VIBRATIONS.* Annual Review of Fluid Mechanics, 2004. **36**(1): p. 413-455.

28. Shames, I.H. and I.H. Shames, *Mechanics of fluids*. Vol. 2. 1982: McGraw-Hill New York.

29. Norberg, C., *Fluctuating lift on a circular cylinder: review and new measurements.* Journal of Fluids and Structures, 2003. **17**(1): p. 57-96.

30. Park, C.H., *On the circuit model of piezoceramics.* Journal of Intelligent Material Systems and Structures, 2001. **12**(7): p. 515-522.

31. Shu, Y.C. and I.C. Lien, *Analysis of power output for piezoelectric energy harvesting systems.* Smart Materials and Structures, 2006. **15**(6): p. 1499.

32. Ng, T.H., *Sensitivity Analysis and Energy Harvesting for a Self-Powered Piezoelectric Sensor.* Journal of Intelligent Material Systems and Structures, 2005. **16**(10): p. 785-797.

33. Shan, X., et al., *Novel energy harvesting: A macro fiber composite piezoelectric energy harvester in the water vortex.* Ceramics International, 2015. **41, Supplement 1**: p. S763-S767.

34. Koumoutsakos, P. and A. Leonard, *High-resolution simulations of the flow around an impulsively started cylinder using vortex methods.* Journal of Fluid Mechanics, 1995. **296**: p. 1-38.

35. Achenbach, E. and E. Heinecke, *On vortex shedding from smooth and rough cylinders in the range of Reynolds numbers 6× 10 3 to 5× 10 6.* Journal of fluid mechanics, 1981. **109**: p. 239-251.

36. Lienhard, J.H., *Synopsis of lift, drag, and vortex frequency data for rigid circular cylinders*. Vol. 300. 1966: Technical Extension Service, Washington State University.